aerospace

MDPI

Article

From Potential Routes to Climate Impact: Assessing the Fleet Transition to Hydrogen-Powered Aircraft †

Gabriele Sirtori [1,*] and Lorenzo Trainelli [2]

[1] Fédération ENAC ISAE-SUPAERO ONERA, Université de Toulouse, 31400 Toulouse, France; lorenzo.trainelli@polimi.it
[2] Department of Aerospace Science and Technology, Politecnico di Milano, 20156 Milan, Italy
* Correspondence: gabriele.sirtori@polimi.it
† This article is a revised and expanded version of a paper published in Sirtori, G.; Trainelli, L. Transient in Operations: From Jet-Fuel to Hydrogen-Powered Aircraft. In Proceedings of the Towards Sustainable Aviation Summit (TSAS 2025), Toulouse, France, 28–30 January 2025.

Abstract

The paper presents a methodology aiming to assess the impact of operations of a short- and medium-range fleet transitioning from jet fuel to hydrogen propulsion, considering the constraint arising from the distribution of hydrogen refueling infrastructures across airports, leveraging on the different performance of the two sub-fleets to obtain the least climate-impacting transition. Hydrogen tankering will enable flights to airports that have no hydrogen refueling capabilities, as long as the destination is within half of the operational range of the selected aircraft, at the cost of a slight increase in fuel burn. The proposed methodology aims to assess said increase, while minimizing the expenditure for hydrogen, and the coverage of a reference network, achievable when considering aircraft performance and assumptions on the availability and cost of hydrogen at various airports. The results of such analysis can be used to determine whether a reduction in the design range of a given aircraft is acceptable. Such a reduction would mitigate the impact that the hydrogen tank has on the sizing of the aircraft and its performance. Depending on the considered scenario, a network potential coverage spanning from 81% to 96% can be achieved. Starting from this result, it is possible to assess the transition of a short-haul airliner fleet from jet fuel to hydrogen propulsion, considering the constraint arising from the distribution of hydrogen refueling infrastructures across airports and the different performances (energetic, environmental and economic) of the two sub-fleets. The aircraft assignment to each route is performed with the objective of minimizing either the energy, the carbon intensity or the fuel cost of the overall network, obtaining different route assignment distributions. The results show that the aviation-induced temperature change can be reduced by up to 57% compared to an all-jet-fuel fleet.

Keywords: hydrogen tankering; hydrogen-powered aircraft; fleet transition; climate impact; operational range optimization; energy efficiency; carbon intensity reduction; infrastructural constraints

Academic Editor: Miroslav Kelemen

Received: 17 September 2025
Revised: 4 November 2025
Accepted: 26 November 2025
Published: 1 December 2025

Citation: Sirtori, G.; Trainelli, L. From Potential Routes to Climate Impact: Assessing the Fleet Transition to Hydrogen-Powered Aircraft. *Aerospace* **2025**, *12*, 1075. https://doi.org/10.3390/aerospace12121075

1. Introduction

Environmental sustainability is the big challenge that commercial aviation is facing and will be facing in the coming decades. In fact, aviation accounts for about 2% of man-made CO_2 emissions and for 12% of transport-related emissions [1]. A technological revolution is therefore essential to achieve the decarbonization of the sector. Among the possible

solutions, hydrogen stands out as one of the most promising options, particularly for short-range aircraft [2,3], which would use hydrogen via direct combustion. Regional aircraft could also use hydrogen recurring to hybrid-electric architectures, in which hydrogen would be used by fuel cells to be converted into electricity [4]; this aircraft category could also recur to thermal hybrid-electric configurations, which could come to market sooner because of a higher Technology Readiness Level (TRL) [4]. The work presented here focuses on short-haul traffic, as this segment accounts for the highest portion of available seat kilometers (ASK) and is expected to achieve entry into service (EIS) sooner than long-haul hydrogen-powered aircraft. The approach presented here could potentially be extended to networks of fuel cell-powered regional aircraft. The momentum on sustainable aviation is also shared with the industry: in fact, there is also an emerging industrial interest in hydrogen-powered commercial aviation, such as Airbus (Toulouse, France) ZeroE [5], targeting short-haul aircraft powered by either fuel cells or hydrogen combustion with an initial target entry into service in 2035 now postponed to 2040, and Universal Hydrogen (Toulouse, France) [6], which, despite financial issues, managed to perform some test flights with a fuel cell-powered aircraft. Additionally, Zeroavia (UK) has recently initiated the FAA certification process for a 600 kW fuel cell to be used on their ZA600 hydrogen-electric engine for regional aircraft with up to 20 seats [7]. Similarly, H2FLY (Stuttgart, Germany) is developing a fuel cell propulsion system currently being tested on Joby's eVTOL (Santa Cruz, CA, USA), while simultaneously working on a more powerful 175 kW version [8]. Research activities and industrial projects also align with political resolutions [9], such as the European Green Deal, which has legally binding targets included in the European Climate Law. The goal is to achieve EU climate neutrality by 2050 through initiatives focused targeting various sectors. The emissions are monitored via the EU Emission Trading Scheme (ETS), which, via a cap and trade mechanism, requires polluters to pay for their greenhouse gas emissions. For what concerns aviation [10], ETS credits, historically awarded for free based on reference past emissions, is seeing the free allocation drop by 25% in 2024 and 50% in 2025, with full auctioning introduced starting in 2026. The emission allowance price (80 €/t_{CO_2}, equivalent to approximately 252 €/t_{Ker}) will push airlines to increase their effort towards decarbonization. Furthermore, starting in 2025, the monitoring and reporting of non-CO_2 effects has begun, based on a model that accounts for aircraft type, route and weather data. Furthermore, the RefuelEU initiative [11], developed in 2023, has the objective of increasing both demand and production in SAF, which enables a significant reduction of CO_2 emissions over the complete fuel life cycle by substantially reducing well-to-tank emissions. Concretely, the regulation forces fuel suppliers at all EU airports to have an increasing-in-time minimum share of Sustainable Aviation Fuel (SAF). Looking outside of the EU, the Carbon Offsetting and Reduction Scheme for International Aviation (CORSIA) prescribes that airlines based in countries that adhere to ICAO monitor and report their emissions due to international flights, in order not to exceed 2020 levels. Currently, participation is voluntary, but it will be mandatory starting in 2027.

Thus, there is a strong regulatory push towards sustainable solutions that can be applied to commercial air transport. This is coupled to several pieces, such as [3,12–19] that focus on developing useful tools for the preliminary sizing of innovative, hydrogen-powered aircraft. These methodologies do not question whether the Top Level Aircraft Requirements (TLARs) should evolve from the current status quo, in order to minimize the impact of the energy carrier switch. Such an analysis needs to be based on thorough analyses that account for the availability of refueling infrastructures across the target network and the performance of the novel fleet, which, while mitigating the environmental impact of air transport, poses new significant challenges. A climate impact analysis can also be performed to optimize the fleet transition. In fact, our previous results [20] show that the

switch to hydrogen causes an increase in the Energy Intensity (EI, that is the energy used to transport one passenger over a distance of 1 NM, measured in MJ/ASNM), highlighting the need to mitigate the impact of hydrogen storage and propulsion on aircraft performance. The energy increase is due to the elongation of the fuselage required to accommodate the cryogenic hydrogen tank (greater wetted surface) and of suboptimal temperatures in the combustion chamber to maintain a suitable Turbine Entry Temperature, both causing an increase in the Thrust Specific Energy Consumption and thus on the overall mission energy.

Starting from these aircraft design results, the work shown in this paper has the ambition to analyze the impact of hydrogen-powered aircraft in real-life operations by addressing operational constraints and climate impact. Some reference networks are assessed in terms of potential route coverage, given a distribution of hydrogen refueling infrastructures at the served airports. A solution to mitigate its sparse availability is tankering, which enables serving airports without such facilities if certain conditions are met. This practice has an impact on economics and in terms of the extra consumption, both considered in this work. Tankering is currently mainly practiced because of economic reasons, as there could be occasions in which taking more fuel at an airport where its price is low might cause savings to the airline, despite an increased fuel consumption because of a higher gross mass. Other instances of application of tankering might be linked to strikes of refueling personnel or limited supply of jet fuel because of pipeline failures; such cases are extraordinary and not considered here. Similarly, hydrogen tankering may offer economic savings, but more importantly, it could enable the operation of hydrogen-fueled flights to destinations that lack a hydrogen refueling infrastructure. In fact, the airline fleet turnover will cause concurrent operation of airliners using either kerosene or hydrogen, with hydrogen refueling infrastructure likely to be introduced initially only at the largest hubs. Smaller airports would probably be involved at a later stage. In particular, the presented methodology allows assessing complete operational scenarios consisting in short- and medium-haul flights out of a reference airport. The analysis gives interesting results in terms of the repartition into operable flights (eventually with partial tankering for economic reasons)—operable with full tankering and not operable routes within the scenario—mostly depending on the design range (DR) of the aircraft. A sensitivity analysis on the DR is performed, to find the best value that enables sufficient network coverage and a mitigation of the increased energy consumption linked to the switch to hydrogen.

The results of potentially flyable routes can be coupled with a fleet replacement model that introduces the transient from a fully kerosene-based fleet to an increasingly hydrogen-powered one. Since, especially initially, the hydrogen fleet will not be big enough to fly all of the routes that it can potentially serve, it is possible to introduce an optimizer that assigns each city pair to either a kerosene or hydrogen aircraft, respecting the fleet ratio (FR), with the objective of minimizing various indicators, such as the overall network energy efficiency, CO_2 intensity or energy cost. The climate impact of the various fleet transition scenarios is evaluated using the Average Temperature Response (ATR) indicator to understand the potential climate impact mitigation offered by the introduction of hydrogen-powered aircraft on a reference network.

Building on what was presented in ref. [21], Section 2 presents a review of the state of the art for fleet transition and airline operation climate impact modeling. Section 3 details how routes that can potentially be served by hydrogen aircraft are identified, given a set of aircraft performance and hydrogen availability distribution at concerned airports. Lastly, Section 4 develops how a fleet transition from legacy kerosene aircraft to novel hydrogen-powered ones can be optimized to minimize the climate impact, computed referring to the ATR indicator, of airline operations over the transition period.

2. State of the Art

The operation of hydrogen-powered aircraft introduces significant challenges that need to be addressed to ensure that a reliable schedule can be carried out, profiting as much as possible from the peculiar performance of the novel fleet. In particular, the route attribution to a legacy or novel aircraft, depending on the route length and on hydrogen refueling availability at the two served airports, is worthy of a thorough investigation, to assess how impactful the novel fleet will be on emissions, operational flexibility and cost. This analysis, covering fleet assignment and the development of hydrogen refueling infrastructures, is extensively developed in this paper, but is also already addressed in the literature. Ref. [22] analyses a portion of Ryanair's operations out of Ireland, with the ambition of assigning specific routes to either a Boeing 737MAX or a hydrogen-powered counterpart, to minimize either the operational cost or the CO_2 intensity of the operations. The attribution, performed using a Mixed-Integer Linear Programming (MILP) solver on Matlab, considers three scenarios, with 0% (baseline), 25% and 50% of the 20-frame fleet to be powered by hydrogen. The fuel burn of the kerosene sub-fleet is estimated using an aircraft performance model based on SUAVE [23] and validated against real-world data from Ryanair-operated flights. Given that Ryanair operates at a constant Cost Index throughout its operations, obtaining a closely matching reference flight profile is possible, which is then analyzed thanks to flight mechanics equations to obtain the fuel burn. The extra energy consumption of hydrogen aircraft, because of a higher Empty Mass and larger wetted surface, is accounted for in the performance analysis of the innovative sub-fleet. The results showed hydrogen planes operating the shorter flights, because of a more contained increase in operational costs. The assumption for hydrogen cost is 3.35 €/kg, whereas Jet Fuel is assumed to cost 0.40 €/kg, plus the ETS price of 80 €/t_{CO_2}. The fleet-wide CO_2 emissions and profit drop by 7.46% and 3.81%, when the hydrogen sub-fleet represents 25% of the total fleet, and 27.41% and 7.63% with half of the fleet composed by innovative aircraft. Furthermore, the two sub-fleets do not show similar aircraft utilization, with innovative aircraft flying less than the legacy fleet. Lastly, an interesting result shows that introducing hydrogen refueling capabilities at Dublin, Liverpool and Glasgow enables an 8.77% reduction in total carbon emissions of the considered operations, highlighting how a smart choice of hydrogen refueling infrastructure can significantly reduce the overall carbon impact of operations.

The work presented in this paper has the ambition of assessing complete short- and medium-haul networks out of selected reference airports; thus, a broader model for the availability of hydrogen refueling infrastructure at various airports is needed, as presented in detail in [24,25]. The first paper thoroughly analyzes different ways of supplying hydrogen to airports, namely on-site production, considering various energy sources, and off-site production, with transport via LH2 or GH2 pipelines. The underlying assumption is that GH2 is always available at a fixed price. The on-site production was identified as the most convenient, at least for larger airports, validating the approach and results of AHRES, our in-house methodology to perform the preliminary sizing of hydrogen refueling infrastructures at airports [20]. Furthermore, the authors assume that large-scale liquefaction, storage, and distribution infrastructure can be deployed where needed, with no major regional constraints or cost escalation—thus treating hydrogen supply and airport refueling networks as readily accessible and fully developed in the study horizon. The second paper presents, among other things, a list of airports and relative expected hydrogen prices and supply methods. The final hydrogen price reflects not just production but the entire logistics, infrastructure, and policy environment around hydrogen supply. The subset of these airports representing the short- and medium-haul destinations out of Milan Malpensa, one of the scenarios considered in this paper, are shown in Figure 1: the circles

represent airports that are equipped with a hydrogen infrastructure according to [25], with the color representing the price of 1 kg of hydrogen, spanning between 1.97 €/kg at Dublin and 2.97 €/kg at Krakow; the black asterisks represent the destinations that are not expected to have hydrogen available.

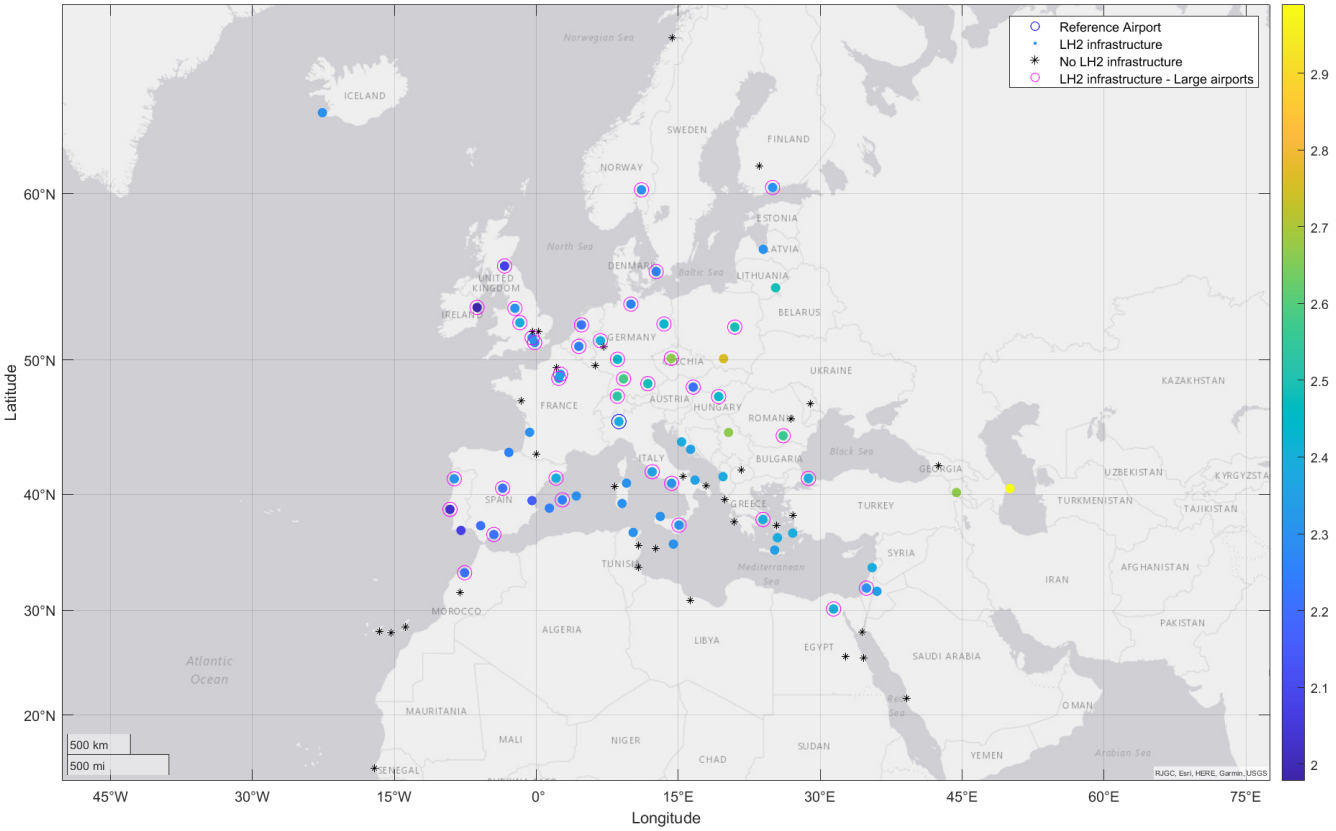

Figure 1. Hydrogen infrastructure availability and price for the short-medium range network out of Milan Malpensa.

Furthermore, an intermediate hydrogen availability scenario is considered, with the infrastructure available only at larger airports (>10 M passengers per year), as shown by the pink circles in Figure 1. This price range for hydrogen at airports is consistent with values presented by other sources for the same time scenario (2050):

- Ref. [26]: 3.45 €/kg for green hydrogen production + 0.52 €/kg for distribution, liquefaction, storage, refueling;
- Ref. [27]: 2.35–3.30 €/kg for production and distribution, liquefaction, storage, refueling;
- Ref. [28]: 2.2 €/kg for production only;
- Ref. [29]: 1.2–2.5 $/kg for production [30] + 1.2 $/kg for distribution, liquefaction, storage, refueling.

A broader review on the topic can be found in [31], which develops a model to quantify the future hydrogen requirements in the aviation sector.

An important metric for the evaluation of the proposed innovative aircraft is represented by their climate impact. A basic evaluation could be carried out by computing the equivalent CO_2 emissions, CO_2e, of the exploitation of the different fleets. Nonetheless, the emissions rates of hydrogen and jet fuel combustion differ significantly; therefore, a more extensive analysis is deemed necessary.

A literature review showed that the ATR, introduced by [32], is a good metric to evaluate the climate impact of aircraft operations; properly modified, the model allows us to evaluate the environmental impact of a fleet transition scenario. In fact, it allows the

computation of the average temperature change due to the aircraft emissions in operation over a given timeframe and the impact due to those substances remaining in the atmosphere once emitted. The formal methodology presented by [32] has been updated to consider a fleet composed of both hydrogen and jet fuel aircraft, with an increasing ratio of the latter, as time advances. The choice of the ATR as a suitable climate metric is also supported by [33], which states that the indicator has been developed specifically for aviation and is flexible enough to account for the assessment of a fleet evolution. Nonetheless, an important variable in the definition of the ATR is the application timeframe, which has a strong impact on the results as it impacts the relevance of short-lived effects compared to long-term effects. The 30-year timeframe was selected because it aligns closely with the duration of the fleet transition being evaluated, and it allows for a thorough assessment of short-term impacts—especially relevant since hydrogen combustion produces no CO_2 emissions, which are known for their long-term environmental effects. Last, it is important to point out that the results of the ATR metric are dependent on the used climate response function. A brief summary of the one used here, as proposed from [32], is now presented in the following. The theoretical definition of ATR_{30} is

$$ATR_{30} = \frac{1}{30}\int_0^{\infty} \Delta T_{Sust,30}(t) \cdot w(t)\, dt, \tag{1}$$

where the function $\Delta T_{Sust,30}(t)$ is determined based on the annual emissions rates for the first 30 years of CO_2, NO_x, H_2O, soot, and sulfate, followed by zero emissions.

The climate impact is estimated considering the emission rates presented in Table 1. For Aviation-Induced Cloudiness (AIC), commonly known as contrail, a radiating factor of $2.21{\cdot}10^{-2}$ W/(m^{2}NM) for jet fuel [32] (value also coherent with data of [34,35]), reduced by 70% for hydrogen [14], is considered. A sensitivity analysis ($\pm$70% from the reference AIC's RF per unit length for kerosene aircraft) on this reduction factor is also introduced in the result section, given the uncertainty on contrail emissions by hydrogen jet engines.

Table 1. Emission indices.

Fuel	Jet Fuel [32]	Hydrogen [14]
CO_2 [kg/kg$_{Fuel}$]	3.16	0.00
NO_x [kg/kg$_{Fuel}$]	$2.08 \cdot 10^{-2}$	$2.34 \cdot 10^{-2}$
H_2O [kg/kg$_{Fuel}$]	1.26	8.93
SO_4 [kg/kg$_{Fuel}$]	$2.00 \cdot 10^{-4}$	0.00
Soot [kg/kg$_{Fuel}$]	$4.00 \cdot 10^{-5}$	0.00

It is also necessary to mention that NO_x emissions are highly dependent on engine type and thrust. The value proposed by [32] is coherent with emissions values stored in the EMEP/EEA air pollutant emission inventory guidebook [36]. To evaluate the climate response, first, it is necessary to compute the radiating factor (RF) for each specie i, with different models for long-lived gases, as expressed in Equation (2a), short-lived pollutants (Equation (2b)), and AIC, as expressed in Equation (2c) below:

$$RF_i(t) = s_i(h)\int_0^t G_i(t-\tau)\cdot E_i(\tau)\, d\tau, \qquad \text{for } i = CO_2, NO_x\text{-}O_{3L}, \tag{2a}$$

$$RF_i(t,h) = s_i(h)\left(\frac{RF_{ref}}{E_{ref}}\right)_i E_i(t), \qquad \text{for } i = H_2O, NO_x\text{-}O_{3S}, Soot, SO_4, \tag{2b}$$

$$RF_{AIC}(t,h) = s_{AIC}(h)\left(\frac{RF_{ref}}{L_{ref}}\right)_{AIC} L_i(t), \qquad \text{for } i = \text{AIC}, \tag{2c}$$

where $G_i(t-\tau)$ represents the temporal decay of the radiating factor of substance i. These factors have been calculated based on the average route length of each sub-fleet during the

analyzed timeframe, assuming a cruise altitude of 35,000 feet. $EI(t)$ represents the emission per species as a function of time, considering the emission indices of Table 1. The factors in brackets represent the RF per unit of emitted species, as shown in Equation (2b), or per unit of distance, as shown in Equation (2c). $s_i(h)$ is the altitude-dependent forcing factor, to account for the different climate impacts of NO_x and AIC, as a function of the emission altitude. In particular, the impact of NO_x is computed considering its short-term effect of ozone production, with a warming effect, and long-term effects of ozone and methane destruction facilitation, with a cooling effect.

The total change of temperature as a function of time is computed by integrating the summation of the normalized RF multiplied by $G_T(t-\tau)$, which represents the two decay modes of thermal response of the Earth system to an energy perturbation, as in Equation (3). The normalized RF is obtained considering each species' efficacy parameter f_i and the RF resulting from a doubling of CO_2, RF_{2xCO_2}:

$$\Delta T(t) = \int_0^t G_T(t-\tau)\left[\sum_i \frac{f_i \cdot RF_i(\tau)}{RF_{2xCO_2}}\right] \mathrm{d}\tau \tag{3}$$

The proper implementation of this methodology has been verified by the application to the same scenario proposed in the reference. The ATR indicator only considers the climate impact linked to the use of the fuel, i.e., tank-to-wake emissions, neglecting the well-to-tank emissions, which vary significantly for hydrogen, depending on the way it is produced [37,38]. It is thus necessary to note that only hydrogen produced by renewable-electricity-powered electrolysis is a viable way to decarbonize commercial aviation, if the entire life cycle of the fuel is considered.

3. Potential Routes for the Hydrogen Sub-Fleet

3.1. Setting the Picture

Given a reference airport equipped with a hydrogen refueling infrastructure, there are five possible operational cases, which depend on the presence of hydrogen refueling infrastructure at the destination airport and on the design range of the aircraft that operates that particular flight. A short route is here defined as a route whose covered distance is less than half of the aircraft's operational range, meaning that the tank has enough capacity to contain hydrogen for both the outbound and inbound flights, with enough capacity for the regulatory reserves for both flights. The two-flight mission profile is shown in Figure 2, detailing the altitude and tank level as a function of time.

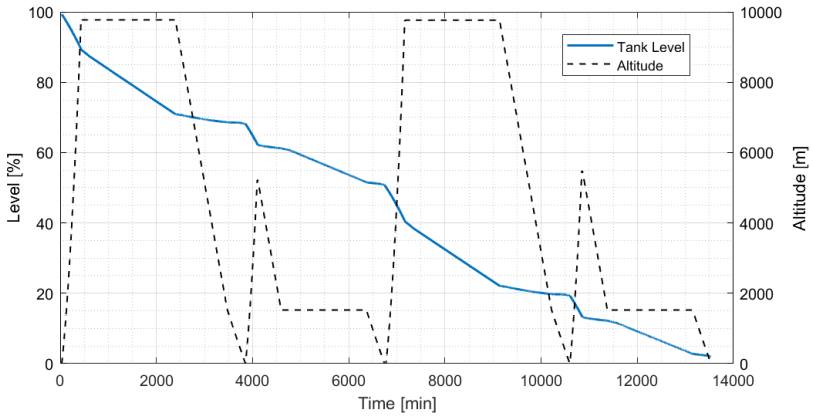

Figure 2. Mission profile for the two-segment short route, with refueling only at the origin.

Instead, a long route covers a distance that is longer than half of the operational range, meaning that the aircraft cannot operate the round trip with fuel only coming

from the origin airport. The operational range is obtained from HYPERION [39], our in-house preliminary aircraft design methodology, for each aircraft that operates a route in the considered scenario. The five operational scenarios are defined as the following five possible types:

1. **Short route with hydrogen refueling infrastructure at destination:** The aircraft can be refueled both at the reference airport and at the destination airport. The quantity of fuel bought at the destination airport is computed minimizing the overall expenditure for hydrogen for the return trip, with an eventual constraint on the additional hydrogen consumption caused by tankering on the outbound leg.
2. **Short route with no hydrogen refueling infrastructure at destination:** The return flight can be operated; all of the hydrogen required to operate the return trip is uplifted at the reference airport.
3. **Long route with hydrogen refueling infrastructure at destination:** The aircraft does not have the capability to operate the return trip only with hydrogen bought at the reference airport. Partial tankering can still happen, should the hydrogen price at the destination airport be significantly higher than that at the reference airport. In any case, it will be necessary to buy some hydrogen at the destination airport.
4. **Long route with no hydrogen refueling infrastructure at destination:** This city pair cannot be operated by the selected aircraft, as it cannot be refueled to operate the return flight.
5. **Destination further than the aircraft maximum range:** The reduction of the design range will prevent the operation of certain flights, whether the destination airport has hydrogen infrastructure or not.

These five possible cases are represented in Figure 3, highlighting that airports that have no hydrogen refueling infrastructure and are further than half of the operational range of the selected aircraft cannot be served with nonstop flights.

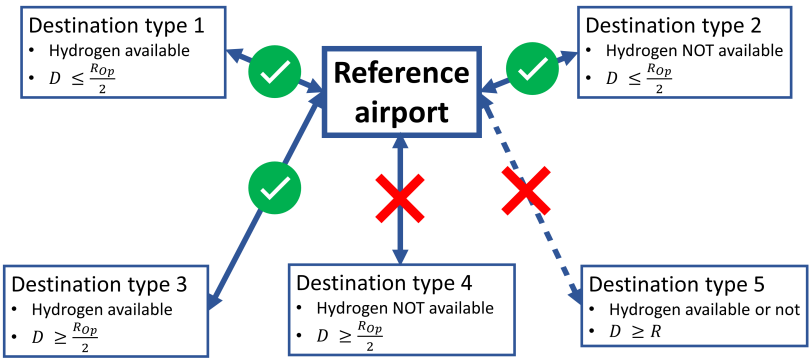

Figure 3. Representation of operational scenarios, with destinations marked in red not serviceable by the hydrogen-powered subfleet.

The developed methodology has the objective of quantifying the impact of hydrogen tankering, in terms of increased fuel consumption, but, more importantly, in terms of improved versatility for the operation of hydrogen-powered aircraft, which can be used to serve some airports that have no hydrogen refueling infrastructure.

3.2. Methodology

Fuel tankering is a practice whereby an aircraft carries more fuel than required for its flight to reduce or avoid refueling at the destination airport, as defined by EUROCONTROL [40]. This practice is currently carried out to reduce the airlines' expenditure for fuel, despite the greater environmental impact caused by increased fuel consumption due to flights being operated with more than the strict necessary fuel amount. For future

hydrogen-powered aircraft, the practice of tankering can also enable operations in airports not equipped with refueling infrastructure, depending on the performance of the aircraft and the distance between the departure and destination airports.

The proposed methodology takes as input aircraft performance, in terms of hydrogen consumption and design range (DR), and hydrogen availability and cost at different airports. Given a series of flights departing from the reference airport, operated by different aircraft with different performance, the code matches each flight with its corresponding operational case, out of the five presented in Section 3.1. For routes of types 2 and 4, the solution is trivial: all of the refueling happens at the reference airport and the city pair cannot be served with the selected aircraft, respectively. For destinations of types 1 and 3, the optimization is based on the minimization of the round trip hydrogen cost, eventually subject to constraints on the maximum percent extra hydrogen burn in case of tankering, and others. Routes of type 5 can only appear if the scenario is run considering aircraft with a reduced DR compared to the real TLAR.

The output shows the total expense for hydrogen at the reference and destination airports, the extra hydrogen consumed because of tankering and how many flights of the considered scenario can be operated considering the hydrogen availability constraint. It is possible to study different hydrogen refueling infrastructure distribution scenarios and the corresponding route coverage, to assess whether it is possible to reduce the DR of the aircraft, allowing for a smaller hydrogen tank to be installed. Thus, this methodology evaluates how much coverage of a given network can be achieved by an aircraft with a varying design range and a set availability of hydrogen refueling infrastructures at the served airports. The second half of the paper builds on this potential coverage to assign each flight to either a legacy kerosene aircraft or to a novel hydrogen one, accounting for a time-varying fleet composition and with an optimization target.

The work introduced here is built based on previous research efforts, most notably in the context of the Clean Sky 2 project SIENA [39], which have led to the development of novel methodologies dedicated to the most fundamental elements at play: the hydrogen-powered aircraft and the airport hydrogen infrastructure sizings.

The first, mainly implemented in the HYPERION tool, provides a procedure for the preliminary sizing of innovative aircraft, including fuel cell propeller-driven airplanes and hydrogen-burning jetliners. HYPERION has been extensively validated and then used to size hydrogen-powered airliners whose TLARs are the same as those of existing aircraft. The second, implemented in the AHRES tool, allows us to preliminarily size the hydrogen production, storage and refueling infrastructure at an airport, given a defined flight schedule. Both methodologies are illustrated in [20]. The present paper represents an example of the investigations allowed by coupling the above-mentioned tools.

Implementation and Mathematical Formulation

The solution is set as a minimization problem, where the cost function is represented by the sum of the hydrogen expense for each return trip i of the analyzed scenario. Thus, the minimum cost for the entire assessed operational scenario comes as the sum of the optima for each round trip. The tool first associates each destination and operating aircraft to the corresponding category, out of the five presented in the previous section.

The methodology takes as main input the scenario schedule, consisting of the list of flights detailing the destination, the distance from the reference airport and the operating aircraft. An aleatory load factor between 55% and 100% is also associated with each flight, to reflect real-life operations.

Aircraft hydrogen consumption

Only short- and medium-haul flights are considered in this study. The most common aircraft that operate such missions have been modeled on HYPERION [20,39], considering the original TLARs: the Airbus A320 family, including the A319, A320, and A321, the Airbus A220-300, the Boeing 737–800 and the Embraer 190. HYPERION outputs the weight breakdown, wing size and span, together with the power characteristics of the jet engine and hydrogen+tank. Conventional, jet fuel-powered aircraft can also be sized to define a baseline case. The inputs needed by HYPERION to perform the initial sizing procedure are specific information regarding the aircraft (payload, crew), its aerodynamics (lift coefficients in different configurations and drag penalties due to landing gears and flaps), jet engine configuration (two or three spools, combustion chamber temperature, fuel), wing sweep angle and other factors. Furthermore, the design mission needs to be characterized so that the aircraft can be sized to satisfy the required performance. HYPERION computes the outputs blending data from statistical regressions and from the modular modeling of subsystems. Based on first principles (i.e., including the thermodynamics description), the turbofan modeling has been implemented and the complete sizing procedure has been successfully validated against existing short-, medium-, and long-range jetliners. For innovative hydrogen-burning jet aircraft, a cross-comparison with literature results targeting a similar design mission, as expressed by its design mission payload and DR, has been performed, with results shown in Figure 4. Given a slightly higher payload and an average DR, the results show HYPERION being conservative in terms of estimated fuel consumption, 20% greater than the average, resulting in a 10% difference in energy intensity per passenger kilometer.

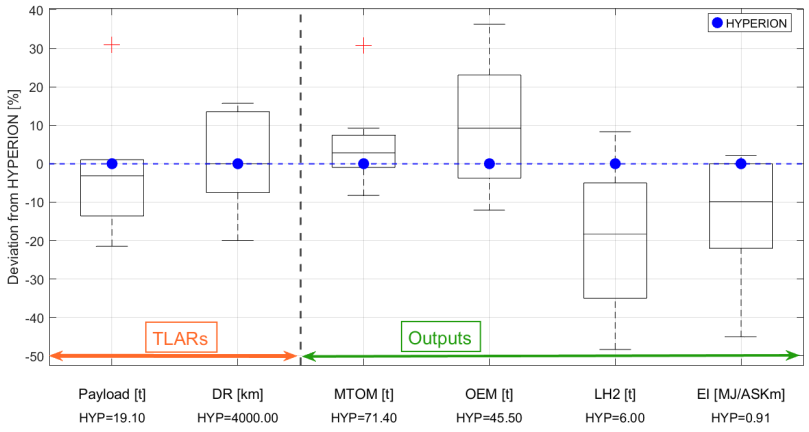

Figure 4. Boxplot of HYPERION input TLARs and consequent outputs for the sizing of an A320-like hydrogen-powered aircraft, in comparison with literature [3,12–19].

As a simplification, all flights in the presented work are considered to be operated by the Airbus A320 or by its hydrogen-powered counterpart, propulsed by hydrogen-burning jet engines. In the case of hydrogen-powered aircraft, the fuel is stored as a cryogenic liquid, with the tank impact on the aircraft sizing and performance properly accounted for. This simplifying hypothesis reduces the computational effort, enables a more straightforward exploration of the design range sensitivity and does not limit the quantification of the impact of the switch to hydrogen, which will be comparable across the aforementioned aircraft. HYPERION gives various information regarding the aircraft layout, performance, and thrust, but the sized aircraft can be deployed on a mission simulator, which allows computing its performance on off-design missions. This feature has been used to obtain look-up tables for the fuel consumption of the aircraft, given a route length and an initial tank level equal to or more than the minimum level, including reserves, needed to complete

the mission. Table 2 shows the hydrogen consumed to perform a flight of a given distance with different initial tank levels, considering a hydrogen-powered aircraft sized according to TLARs matching the performance of the Airbus A320. The values reported on the diagonal of the matrix show the amount of hydrogen required to perform the mission with an initial filling equal to the amount of fuel needed for the mission and 5% of the reserves, whereas by moving to the right, the required hydrogen increases with the initial filling of the tank.

Table 2. Hydrogen consumption as a function of flight distance and initial tank level for the A320H with 100% payload.

Tank Level [%]	17.1	22.5	33.4	44.5	56.72	67.1	78.54	90.4	100
Distance [km]	Fuel [kg]								
200	406	408	414	420	427	431	437	444	448
500		717	722	728	734	740	746	752	756
1000			1356	1367	1377	1386	1397	1407	1417
1500				2001	2018	2031	2046	2060	2074
2000					2654	2673	2692	2711	2728
2500						3313	3333	3360	3379
3000							3976	4003	4029
3500								4648	4677
4000									5323

Such tables have been obtained for different payload levels, from 55% to 100% with a 15% step. A linear interpolation across them is performed to obtain the fuel consumption table associated with the payload level of each route. Then, a proper Non-Linear Least Squares Method [41] allows us to estimate the fuel consumption for flight distances longer than 500 km. For shorter flights, linear interpolation is used.

Minimization problem

The minimization function is shown in Equation (4):

$$C = \sum_{i=1}^{N} (C_{H2,Origin} F_{Origin} + C_{H2,Dest} F_{Dest})_i \tag{4}$$

The objective function is subject to some constraints that vary from case to case. The most interesting are the ones for case 3, presented in Equation (5).

$$\begin{cases} F_{Req} + F_{Div} R_{Div} \leq F_{Origin} \leq T_{aircraft} \\ 0 \leq F_{Dest} \leq F_{Req} + F_{Div} R_{Div} \\ 2F_{Req} + 2F_{Div} R_{Div} \leq F_{Origin} + F_{Dest} \\ F_{Origin} - F_{C(D,F_{Origin})} + F_{Dest} - F_{C(D,F_{Origin} - F_{C(D,F_{Origin})})} + F_{Dest} = 2F_{Div} R_{Div} \\ \dfrac{F_{C(D,F_{Origin})} - F_{Req}}{F_{Req}} \times 100 \leq T \end{cases} \tag{5}$$

where

- C is the total fuel price for the scenario and represents the objective function [€].
- $C_{H2,Origin}$ is the fuel price at the airport of origin [€].
- $C_{H2,Dest}$ is the fuel price at the destination airport [€].
- F_{Origin} is the fuel amount carried from the airport of origin [kg].
- F_{Dest} is the fuel amount carried from the destination airport [kg].
- F_{Req} is the minimum (i.e., no tankering) required fuel amount to fly each leg of the round trip. It is computed by interpolating the diagonal of Table 2 [kg].

- F_{Div} is the fuel amount required to perform one diversion [kg].
- R_{Div} is the diversion rate. This is a surrogate to account for the reserve fuel. Rather than accounting for R_{Div}% of flights using the full reserve fuel, all flights are considered to use R_{Div}% of the reserve fuel. This factor is equal to 5% for the considered scenario [%].
- $T_{aircraft}$ is the aircraft maximum tank capacity [kg].
- T is the limit threshold set on the extra fuel burn [%].

The first and second equations of Equation (5) represent the lower and upper bounds on F_{Origin} and F_{Dest} whose satisfaction automatically satisfies the third equation. The fourth and fifth equations introduce the nonlinearity linked to the fuel consumption as a function of distance and initial tank level. In the equality constraint, the remaining fuel at the end of the round trip is imposed equal to the quantity $2F_{Div}R_{Div}$. This constraint is used to compute the optimal fuel weights to be carried from the airports, while accounting for the diversion fuel amount as well. The last inequality constraint ensures that in case the first flight of the round trip carries more fuel than the required amount, the extra fuel burn due to the increase in fuel weight is limited by the factor T, set equal to 1% for the presented results.

3.3. Results for Potential Routes

This chapter details the results obtained from the application of the methodology to different scenarios, with the objective of assessing the extra fuel burn linked to tankering and the coverage of a given route network, given aircraft with different DRs.

3.3.1. Definition of the Scenarios

The methodology has been applied to various short-haul scenarios in which, as a simplifying hypothesis, all flights have been considered to be operated by the various Airbus A320 hydrogen-powered counterparts, sized with HYPERION. Particularly, all the TLARs remained unchanged, except for the design range at maximum payload, which changed from the original 3770 km to 4000 km, 3000 km and 2000 km. A further version, based on a DR equal to 2450 km, has also been considered, as it corresponds to the maximum round trip range of 981 km, a value that represents the average stage length for European flights in 2020, as pointed out by EUROCONTROL [42]. An objective design range of 2000 km has also been identified for the Horizon Europe EFACA project [43], which, among others, aims to develop a 150-seat hydrogen-powered aircraft, showing how a reduction in the design range compared to current levels is a valid pathway. Note that the mentioned ranges are the true ranges, as a 150 km diversion and 30 min of loiter are also considered. Information resulting from the preliminary sizing of the different aircraft, relevant for the current analysis, is shown in Table 3.

Table 3. Data for aircraft with modified DR.

Aircraft	Real TLARs	DR4000	DR3000	DR2450	DR2000
Design Range [km]	3770	4000	3000	2450	2000
Max RT Range [km]	1650	1720	1250	981	760
LH_2 tank capacity [kg]	5926	6131	4512	3706	3074
Reserve hydrogen * [kg]	544	551	535	528	522
Reserve hydrogen [%]	9.5	9.0	11.9	14.2	17.0

* Reserve including 150 km to alternate airport and 30 min of loiter.

The methodology has first been applied to Milan Malpensa for the schedule of 18 September 2023 (busiest day of the year 2023), consisting of 260 short- and medium-haul flights. Figure 5 shows the design range and the maximum round trip range out of Milan Malpensa for aircraft sized with 2000 km, 3000 km and 4000 km DRs. The curves

corresponding to real aircraft and the 2450 km design range are not shown here for better clarity, as the former almost coalesces with the green curves and the latter is halfway in between the blue and red circles, in a region in which the Mercator distortion is not yet very pronounced.

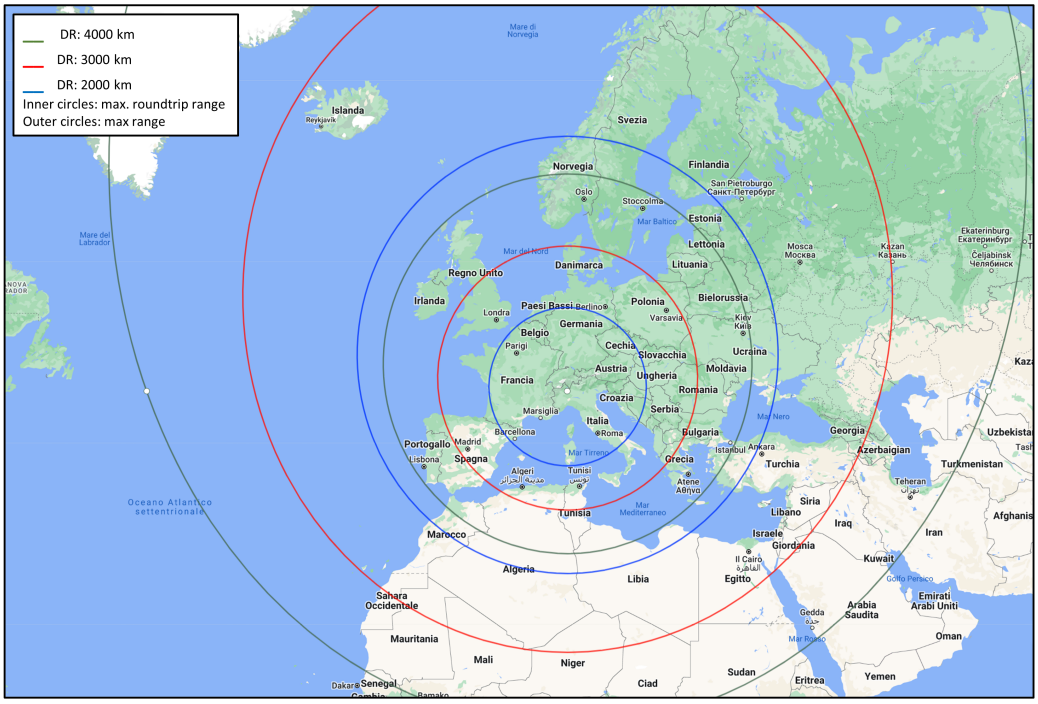

Figure 5. Design range (outer circles) and maximum range for single refueling return trips (inner circles) for aircraft with a 2000 km (blue), 3000 km (red) or 4000 km (green) design range.

Looking at the curves, it is clear that a 3000 km DR aircraft (red circle) covers all of Europe from a very central airport as Milan Malpensa, making such a DR sufficient for European operations, assuming a good availability of hydrogen refueling infrastructures. The maximum range for single refueling return trips associated with the 3000 km design range also offers a decent coverage of central Europe.

This initial overlook shows how the location of the reference airport impacts how limiting the chosen DR and associated maximum range for single refueling return trips are. For this reason, it was decided to assess how the same preliminary-sized aircraft behaves when deployed on other scenarios, namely the short- and medium-range flights of Amsterdam Schiphol (schedule of 5 October 2023, 566 flights), Paris Charles de Gaulle (23 August 2023, 473 flights) and a more decentralized airport such as Lisbon (17 May 2024, 223 flights). The considered schedules cover the busiest day of the year 2023, as shown by EUROCONTROL data [44] at these European airports. Amsterdam and Paris have been selected as they are the largest airports in the EU. Milan Malpensa has been selected as two important stakeholders—the airport operator, SEA [45], and one of the most present airlines, easyJet (Luton, UK) [46]—have shown significant interest in adopting sustainable hydrogen-based solutions to make air transport greener. The Portuguese scenario has been included to assess a case study that could expose the weakness of the proposed methodology when applied to decentralized airports. Furthermore, the SAS (Kastrup, Denmark) short-haul network out of their three main hubs (Copenhagen, Oslo and Stockholm, 30 September 2024 with 324 flights) and the easyJet schedule out of Paris, London, Milan, Berlin and Amsterdam (30 September 2024 with 539 flights) have been assessed, because of a mainly domestic—especially with short routes— network and public interest in hydrogen air-

craft [46], respectively. Precise information regarding the schedule, including frequency and operating aircraft was obtained from the API Flight Labs [47].

3.3.2. Milan Malpensa

The international Milan Malpensa Airport (LIMC), Italy, is taken as the reference airport for the results presented here, with a reference hydrogen price set equal to 2.39 €/kg. All flights have been simulated considering the Airbus A320-like hydrogen aircraft with the original design range and with five other design ranges. It is particularly relevant to mention that an aircraft designed with a 2450 km design range has been considered, as it enables a maximum range for single refueling return trips equal to the average length of European sectors, which is 981 km [42]. This aircraft has also been deployed on an intermediate hydrogen distribution scenario, which sees only airports with more than 10 M yearly passengers having hydrogen refueling capabilities. The resulting route categorization for each assessed scenario is presented in Figure 6.

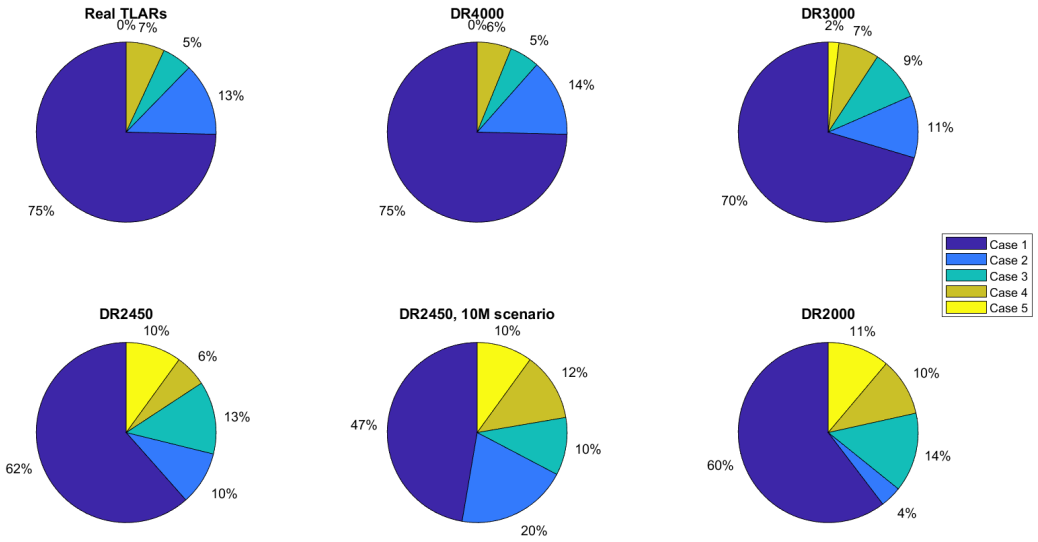

Figure 6. Route categorization at Milan Malpensa with aircraft with different design ranges.

Routes in yellow (dark and light) are the ones that cannot be operated given the particular coupling of aircraft performance and hydrogen distribution scenarios. There is almost no difference between the real TLAR and the 4000 km DR scenarios with 7% and 6% of not operable flights, respectively, as the latter sees aircraft with a slightly larger DR, making a few flights move from category 4 to category 2. The reduction in the DR to 3000 km, 2450 km and 2000 km causes, as expected, the insurgence of flights belonging to category 5 and an overall increase in flights that cannot be operated, adding up to 9%, 16% and 21%, respectively. It is also interesting to notice the important impact of having only large airports (>10 M passengers per year) being equipped with hydrogen refueling infrastructure; in this case, up to 22% (compared to 16%) of flights are not operated. Given these results, it might seem that the reduction in the design range of hydrogen aircraft might be too constraining for real-world operations, given that between 6% and 22% of flights need to be canceled. Nonetheless, this analysis concerns the first generation of hydrogen-burning jet aircraft, which will be operating side by side with current kerosene airplanes, such as the Airbus A320NEO and Boeing 737 MAX families, able to take up those missions that novel hydrogen planes cannot operate. In fact, as suggested by [48], planes have a 30-year lifespan; historically, the plane retirement age has not been affected by more stringent air quality and noise regulations, but only, by a sudden increase in fuel prices. It

will be necessary to evaluate more precisely if the change of energy source affects the fleet turnover dynamics.

Tankering in itself is more of an operational aspect, rather than something usually considered in the pre-design phase; nonetheless, the results of this analysis, in terms of design range associated with the operable percentage of the existing flights of the considered schedule, could be used as an input to perform an educated reduction in the DR, before the aircraft project is finalized. This is extremely relevant, as the design range of a hydrogen aircraft is strongly coupled with the sizing of the aircraft itself. In fact, a longer design range causes a longer hydrogen tank, which in turn causes a further elongation of the fuselage, deteriorating the aerodynamic performance of the aircraft and thus its energy efficiency. Instead, the coupling between aircraft sizing and design range is not nearly as strong for conventional jet fuel-powered aircraft, as generally, the wing is sized to guarantee a certain level of low-speed performance, making enough volume for the fuel tank available.

Clear evidence of this can be found in Figure 7, which represents the normalized hydrogen consumption for all and only the flights that can be operated by DR2000 (79% of the flights), considering a case in which tankering is applied (blue bars) or not (orange bars, assuming that hydrogen is available everywhere). The reference fuel consumption comes from the operations of the aircraft with the real-range TLAR, with tankering. Similarly, Figure 8 shows the normalized hydrogen cost, again considering tankering and no tankering, for all and only routes operated by DR2000 and using the aircraft with real TLARs as a reference. The normalized hydrogen consumption and cost for the scenario that only considers large airports to be equipped with hydrogen refueling infrastructures is not shown in these plots, as its results are not comparable, as both the aircraft performance and the hydrogen accessibility vary in this case study.

There are a few key messages shown by Figures 7 and 8:

- Tankering causes an increased fuel consumption by 0.1% on the complete scenario for all DRs, but reduces the cost linked to fuel acquisition by 0.2%; these results include a hard 1% limit on extra fuel consumption for those routes in which tankering is only an economic mean and not the enabler of the route.
- The reduction in the DR can reduce by up to 7% the hydrogen consumption and the associated cost.
- Even a marginal range increase, for example, going from 3770 km to 4000 km, causes a 0.8% increase in cost and fuel consumption.

The percentile reductions might seem trivial and not worth the limited flexibility of the aircraft, but reducing the design range from the real value to 2450 km allows saving up 27.3 t of hydrogen daily (less on not peak days of traffic) only for short- and medium-range flights in and out of Milan Malpensa, resulting in savings of 64 k€.

Furthermore, the reduction in the design range allows for a decrease in the difference between the Payload-Range Energy Efficiency (PREE) of the conventional Airbus A320 and those of the various hydrogen-powered counterparts. The PREE, computed here on a 981 km mission, is defined as follows in Equaiton (3):

$$PREE = \frac{m_{pl} R g}{m_{Fuel} e_{Sp}} \tag{6}$$

where m_{pl} represents the payload mass, R the range, m_{Fuel} the fuel mass and e_{Sp} the fuel lower heating value. The PREE increases by 5.5%, reducing the DR from the real value to 2450 km. However, it still remains 15.5% lower than that of the conventional aircraft, showing the impact of the hydrogen integration into the aircraft.

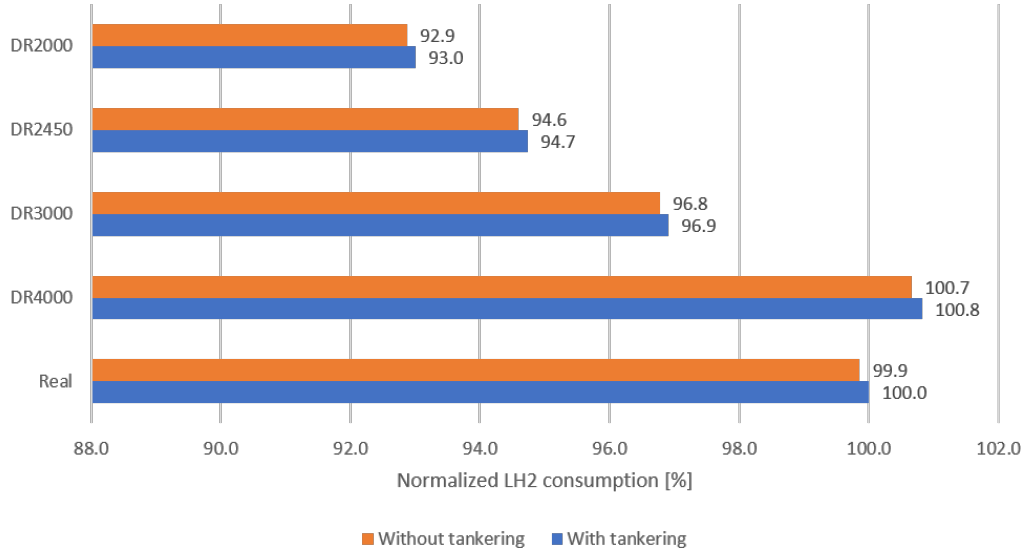

Figure 7. Normalized LH_2 consumption.

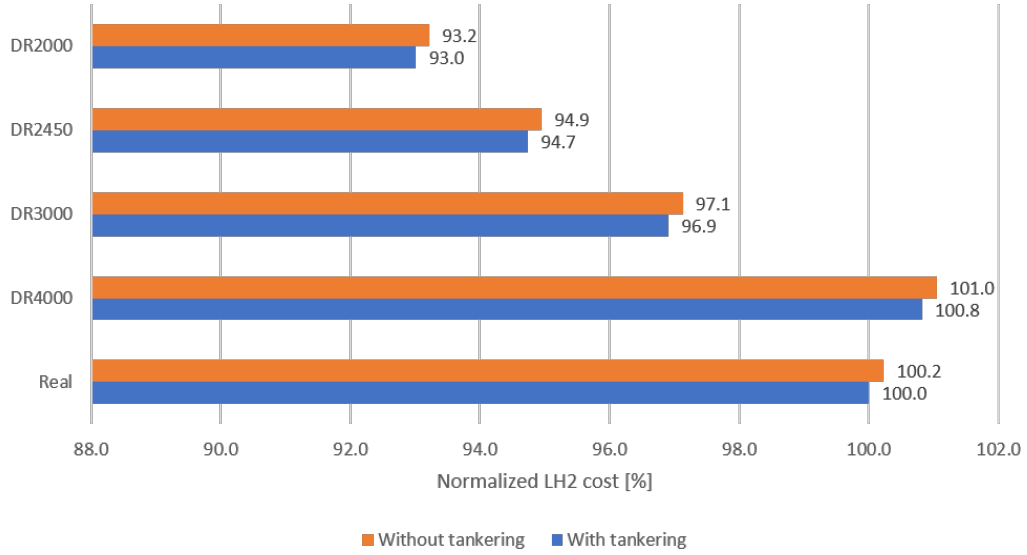

Figure 8. Normalized LH_2 cost.

3.3.3. Other Airports

The same methodology has also been applied to the other aforementioned scenarios. Figure 9 shows these results, in comparison with Milan Malpensa, in terms of route categorization considering the DR2450 aircraft, which is therefore the one sized considering the average length of European flights as the maximum flyable return distance.

Amsterdam and Paris see a route categorization distribution similar to that of Milan Malpensa, with approximately 60% of flights belonging to Category 1 and 11% of flights that cannot be operated, compared to 16% for Milan Malpensa. A completely different situation appears for the Lisbon scenario, in which only 36% of flights are "short" (cat. 1 and 2) and 19% of flights cannot be operated. This result shows that less central airports have fewer "short" routes and more routes that cannot be operated, either because of the lack of hydrogen refueling infrastructures or because of the more limited aircraft performance. The results are also confirmed by the analysis of two operators' flights, with SAS seeing only 4% of non-flyable routes, thanks to its domestic-heavy network, and easyJet with 12%, aligning itself to central airports which see similar operations.

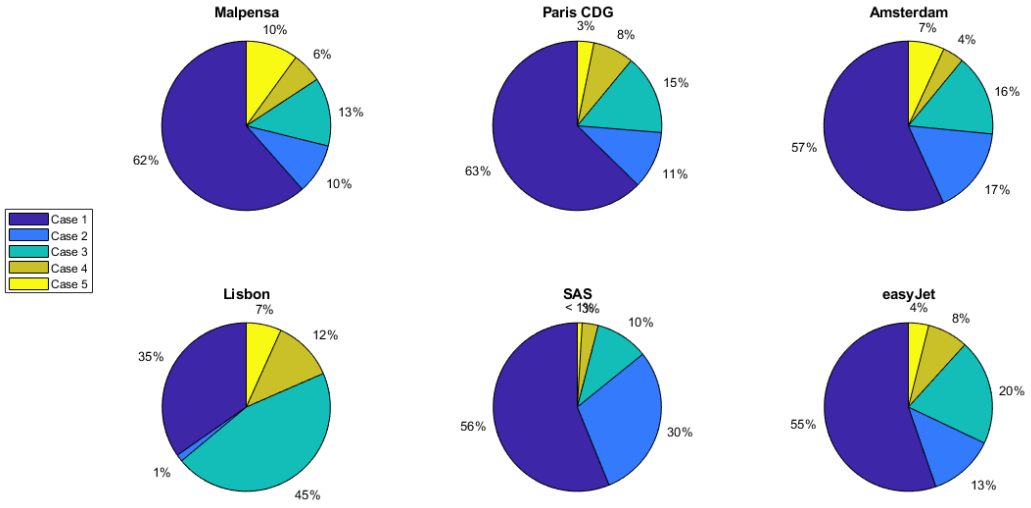

Figure 9. Route categorization at various airports with aircraft with a 2450 km design range.

3.3.4. Sensitivity Studies

It is also interesting to perform a sensitivity analysis on the hydrogen price difference between the reference and destination airports. The hydrogen price at the reference airport is set equal to 2.39 €/kg. Considering that hydrogen is available at both sites, a maximum of 2% extra hydrogen consumption over the round trip is set to mitigate the increased energy consumption. This threshold is twice as large as that used to assess the complete scenarios, to obtain more insightful results. Figure 10 shows the results in terms of net savings, tankering percentage, and extra fuel burn, as a function of flown distance and considering a price difference spanning from 1% to 5%.

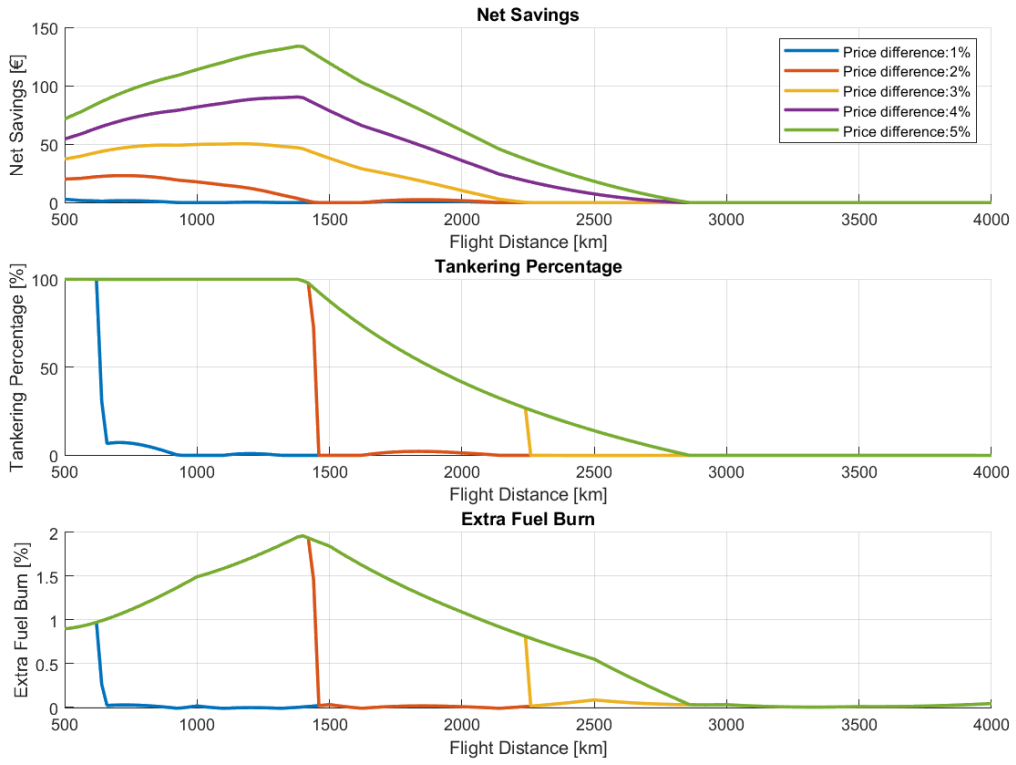

Figure 10. Net savings, tankering percentage and extra fuel burn for the 4000 km range aircraft, as a function of flight distance for a varying price difference between the reference and destination airports.

No minimum net saving has been imposed for the sensitivity studies. If the threshold used in the complete scenario simulations (30 € on each return trip) is considered, it is clear that a 1% or 2% price difference does not warrant tankering, if only for economical reasons. The tankering percentage stays equal to 100% up until the maximum round trip range for higher price differences. It decreases slowly because of the tank size limit, but drops to zero as soon as the net savings would become negative, meaning that the increased fuel consumption would cost more than the saving enabled by the cheaper fuel. Intuitively, higher price differences enable higher economic savings. The distance corresponding to the maximum saving increases with the hydrogen price difference.

4. Optimal Fleet Transition

4.1. Fleet Transition Optimization

The preceding analysis identifies routes that could potentially be served by hydrogen-powered aircraft. However, transitioning from an entirely kerosene-based fleet to one partially powered by hydrogen will require time, as the typical lifespan of an aircraft goes up to 30 years, with hundreds of new jet fuel planes still being delivered every year, resulting in a gradual adoption of newer technologies. The projected share of hydrogen-powered aircraft over time, based on the fleet replacement model developed by [49], is depicted in Figure 11. The introduction of hydrogen-powered aircraft is anticipated to commence in 2035, aligning with the expected EIS date of Airbus' ZeroE family.

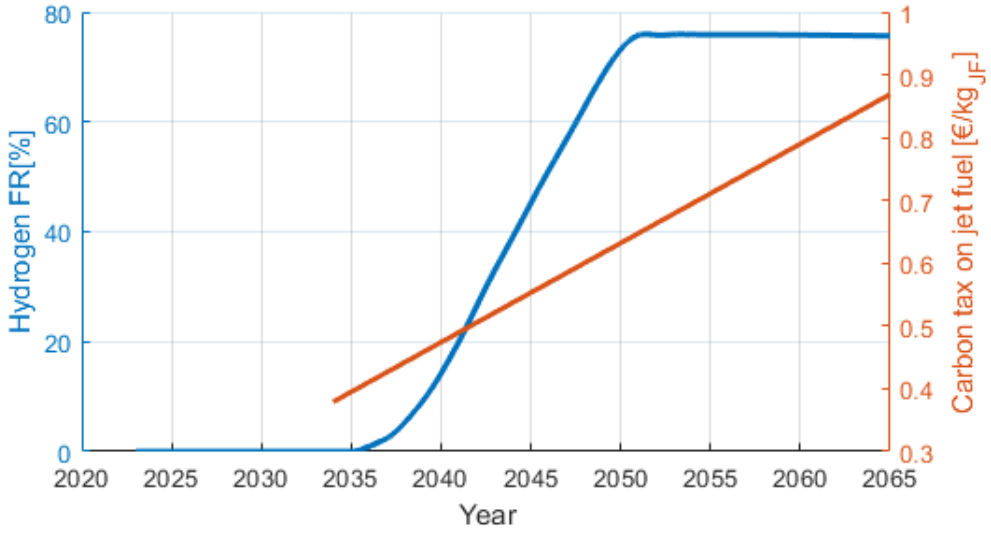

Figure 11. FR of hydrogen aircraft in fleet (blue) and carbon tax on jet fuel (red) as a function of time.

The model has been adapted to have a maximum of 77% of hydrogen aircraft in the fleet to have a margin with the worst-case scenario of routes that can be operated by hydrogen aircraft; see Section 3. The cited gradual phase-in strategy accounts for factors such as production capacity, infrastructure development for hydrogen refueling, and regulatory approvals, all essential in supporting a large-scale transition to hydrogen-powered aviation.

Integrating the potential routes results with the fleet replacement model enables assessing the fleet transition over a specified timeframe in terms of aircraft route coupling and environmental impact. Since more routes and corresponding flight hours will be potentially suitable for hydrogen aircraft than available hydrogen-powered planes will be in the fleet, an optimization framework can be established to assign each route to either a jet fuel or hydrogen aircraft, year to year as the hydrogen fleet ratio grows. This optimization can target one of the three proposed objectives:

1. Minimize the fuel expenses of the network, measured by the Fuel Cost per Available Seat Kilometer (FCASK);
2. Minimize the overall energy intensity of the network;
3. Minimize the total CO_2 intensity of the network.

This optimization problem lies in the category of operations research for scheduling, which can be solved by resorting to the linear integer programming methodology, such as the one used in [50]. Such optimization is crucial for operations-intensive businesses such as airlines, as it provides many opportunities for efficiency improvements, given a fixed set of assets, the fleet and the targeted network [51]. The optimization aims to minimize one of the targeted indicators, as follows:

$$minimize \sum_{i=1}^{N_{Flights}} (x_i \cdot P_{H2,i} + (1 - x_i) \cdot P_{JF,i}), \tag{7}$$

where x_i equals 1 if the i^{th} flight is assigned to a hydrogen-powered flight or 0 if the operating aircraft is kerosene-powered. $P_{H2,i}$ and $P_{JF,i}$ represent the target parameter of the optimization (cost, energy intensity or CO_2 intensity) for the i flight for the two sub-fleets. The cost model includes the energy acquisition cost (for jet fuel, fixed at 0.816 €/kg, and for hydrogen, based on the geographical scenario presented in Section 2). Furthermore, a linear tax on carbon emissions, hereon indicated as carbon tax (CT), is considered, spanning from 125 €/t_{CO2} in 2035 to 275 €/t_{CO2} in 2065 [52], shown in orange in Figure 11. This basic cost model does not account for the evolution of fuel prices, which cannot be evaluated proficiently as they depend on many external factors, such as policies, geopolitical crises and several other external factors. Furthermore, other operating costs, such as crew wages and aircraft acquisition costs, are not considered.

The proposed solving strategy does not aim to develop a precise schedule–fleet assignation, but rather to understand the optimal general assignment of routes considering the availability of hydrogen at the served airports. Thus, the only imposed constraint, changing for every year of the transition, aims to guarantee that the hydrogen fleet operates the portion of the schedule that is coherent with its relevance in the fleet, as follows:

$$\sum_{i=1}^{N_{Flights}} (x_i \cdot T_i) = FR \cdot \sum_{i=1}^{N_{Flights}} T_i, \tag{8}$$

where T_i represents the time for the return trip to the i^{th} destination, also considering the time required for turnarounds, and FR represents the hydrogen fleet ratio at year y, as shown in Figure 11. Therefore, each assigned flight uses some of the total flight time allocated to either the hydrogen or jet fuel fleet. There are no constraints regarding the sequence of flights, meaning that there is no verification of the exact flight schedule to ensure a specific flight is operated by an aircraft based on its departure time and the arrival time of the preceding flight it operated. Also, constraints due to time slots, which are particularly important for airline operations, especially at larger airports, are not considered either. Passenger spillover, caused by a too-small operating aircraft compared to the traffic level on a specific route, is not evaluated in this analysis, as no real traffic data are available. For this reason, the assumption that all considered flights are operated by the Airbus A320 or by its hydrogen counterpart is not reductive, as it is expected that the impact of hydrogen on short-haul aircraft will be similar for different sizes, i.e., on different aircraft of the A320 family. Thus, the presented optimizer indicates the best set of routes to be flown by hydrogen aircraft in a given network, from a technical point of view accounting for operational constraints for novel sustainable aircraft. Overlying these results with a

normal capacity-based network planner will make it possible to also detail what aircraft size operates each flight, to adapt capacity to maximize the revenue.

4.2. Results

4.2.1. Fleet Transition

The results of the optimization can be expressed by the definition of the average route length assigned to jet fuel and hydrogen aircraft and the corresponding distribution. Further relevant indicators are the sub-fleet and fleet-wide CO_2 intensity, energy intensity and FCASK. In fact, these three indicators provide a good analysis of the fleet performance in terms of environmental impact, energy efficiency, and cost considering the time-dependent hydrogen FR.

The following details results for various simulations of the Milan Malpensa case; the same approach can be used for any of the other scenarios introduced in Section 2.

The first set of results, presented in Figure 12 details the time evolution of the relevant parameters, in a scenario in which the design range of the hydrogen aircraft is the same as that of the reference jet fuel aircraft. The shown results include optimization of the FCASK and energy intensity without the CT, as well as the optimum FCASK results considering the CT. The results that minimize the CO_2 intensity are very similar to those targeting minimum FCASK and, thus, are not shown for readability. In these simulations, the only constraint limiting the novel aircraft operations is the availability of hydrogen at the destination, especially for longer routes. The optimization accounts for the intrinsic performance difference (environmental, energetic, or economic), differentiating the two sub-fleets.

For what concerns route attribution, the two scenarios without the CT show similar results, with slightly shorter routes assigned to hydrogen aircraft in the minimum energy intensity case. A more significant difference is seen if a carbon tax is introduced, which causes a reduction in the length of missions flown by jet fuel aircraft. Reducing the average flown distance forces the legacy fleet to operate more sectors, thus increasing the total turnaround time (30 min per segment) assigned to that sub-fleet. Since each sub-fleet total annual in-service hours are fixed, shorter missions lead to a larger share of time spent on the ground for turnarounds. As a result, the sub-fleet contributes less to fleet-wide performance indicators. The time history of CO_2 intensity shows very similar results for the three optimal solutions, with the average indicator dropping linearly as the hydrogen FR increases. For what concerns the energy intensity, the biggest difference is seen during the transient, showing a higher energy intensity for the scenario that targets minimum cost with CT. It is also important to point out that the average energy intensity increases by approximately 14%, because of the lower efficiency of hydrogen aircraft. The FCASK sees a 20% increase following the introduction of hydrogen aircraft for the two scenarios that do not consider the CT. In the CT Scenario instead, the FCASK remains almost constant over time, 40% higher than the initial FCASK, computed without considering the CT. If we consider hydrogen aircraft with a 2450 km DR, the final fleet-wide energy intensity is equal to 0.82 MJ/ASkm, compared to 0.86 MJ/ASkm in the previous case, showing the beneficial impact of the reduction in the design range of the novel aircraft. The CO_2 intensity has instead similar values both with the real and reduced design range hydrogen fleet. The obtained values are comparable to the data available in the literature. In fact, Icelandair posts an FCASK of 0.022$/ASkm [53]. The CO_2 intensity computed for the overall fleet by [22] is 0.6268 kg/ASkm for the baseline scenario, 0.5290 kg/ASkm and 0.3402 kg/ASkm for an FR of 16.6% and 44.4%, respectively, if recomputed as the ratio of flown hours of the two sub-fleets. The energy intensity of the Airbus A320neo is equal to 0.7517 MJ/ASkm, considering a cabin of 180 passengers, with an expected 15% increase for hydrogen jet aircraft, as indicated in [12].

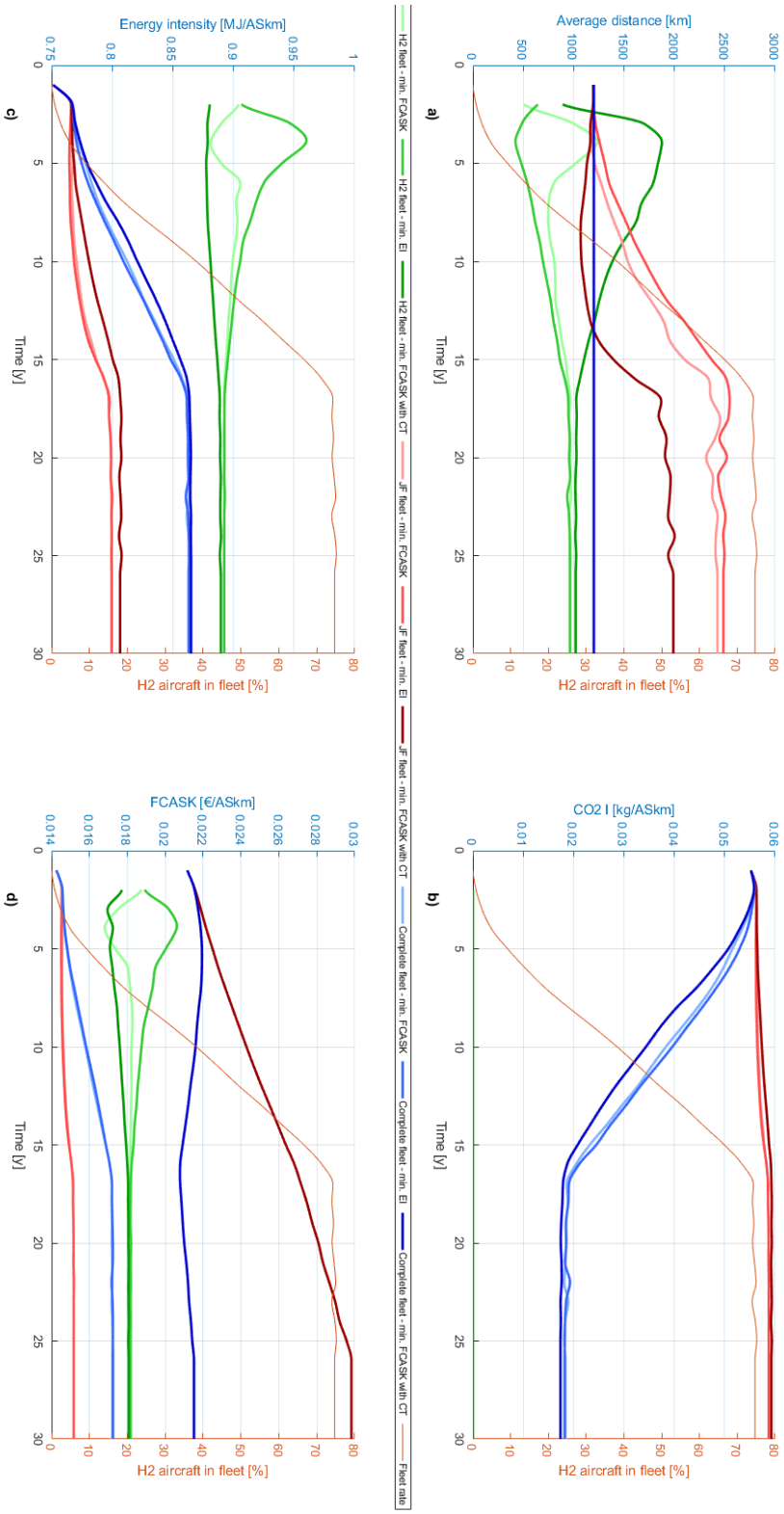

Figure 12. Evolution for the average distance (**a**), CO_2 intensity (**b**), energy intensity (**c**) and FCASK (**d**) as a function of time, hydrogen aircraft sized with the original design range.

Figure 13 details how the routes are distributed among the two sub-fleets, depending on the target indicator. Results obtained minimizing the FCASK and CO_2 intensity are very similar, as in both cases, the hydrogen fleet is assigned to routes whose length is close to the maximum design range of the aircraft, whereas the minimum energy intensity solution

sees the hydrogen flights taking up only short flights, thus minimizing the importance of its flown hours in the complete network.

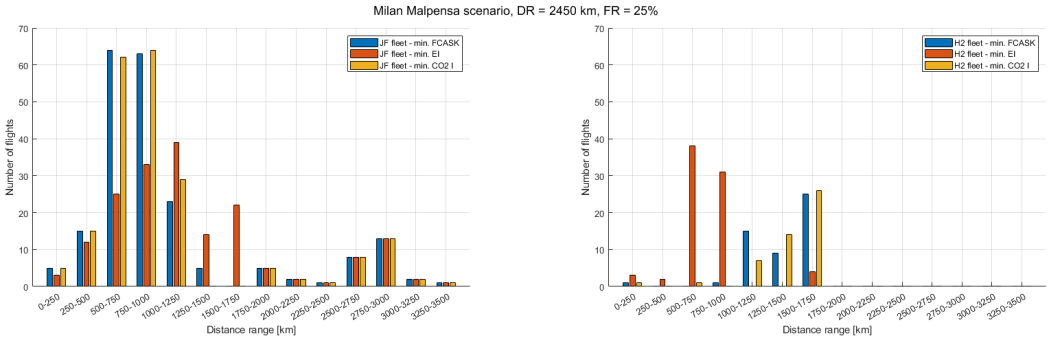

Figure 13. Route length distribution for the 25% FR, DR2450, with CT.

4.2.2. Climate Impact Evaluation

The climate impact of the different scenarios has been assessed using the methodology presented in Section 2, targeting only tank-to-wake emissions for both kerosene and hydrogen. This analysis accounts for all climate-altering emissions, including their latency in the atmosphere, allowing for a broader analysis than just direct computation of CO_2 emissions. The yearly jet fuel and hydrogen consumption, needed as input to compute the climate impact, depends on the hydrogen fleet ratio. The collected daily schedules are extrapolated to estimate yearly fuel consumption by multiplying the daily fuel and hydrogen usage by 365 and applying a corrective factor. This factor accounts for traffic seasonality and is derived from monthly movement data at the reference airports or bases of the carriers under consideration [54]. Furthermore, a yearly increase in traffic of 2.2% [55], assuming a fixed average stage length, is introduced, to account for the expected traffic growth and consequent emissions. The results are presented in Table 4.

Table 4. ATR_{30} results for the different study cases for the Milan Malpensa airport, with the same color code used in Figure 12.

	Real DR						DR2450					
	No CT			CT			No CT			CT		
	1	2	3	1	2	3	1	2	3	1	2	3
ATR_{30Ref} $[10^{-4}\text{K}]$	2.77											
ATR_{30JF} $[10^{-4}\text{K}]$	1.05	1.07	0.943	0.943	1.07	0.943	1.02	1.04	0.943	0.943	1.04	0.946
ATR_{30H2} $[10^{-5}\text{K}]$	2.27	2.20	2.43	2.43	2.20	2.43	2.27	2.20	2.40	2.40	2.20	2.40
$ATR_{30Trans}$ $[10^{-4}\text{K}]$	1.27	1.30	1.19	1.19	1.30	1.19	1.24	1.27	1.18	1.18	1.26	1.19
$\Delta_{\Delta T}$ [%]	−54.1	−53.4	−57.3	−57.2	−53.4	−57.3	−55.2	−54.4	−57.4	−57.4	−54.5	−57.3

The results show a significant reduction in the overall climate impact from tank-to-wake emissions, evaluated as the variation of temperature measured by the ATR_{30} indicator, induced by the transitioning fleet, compared to the baseline, up to −57% depending on the case. Moreover, incorporating the CT enables a further reduction in climate impact compared to the corresponding scenario without it. The least reduction of the ATR_{30} is consistently obtained by the solutions that minimize the energy intensity, as those favor the operation of legacy jet fuel aircraft. Conversely, the solutions for optimal FCASK And CO_2 intensity are equivalent, one to the other, in the simulations that include the CT, with a slight deterioration for the min. FCASK if the tax is not considered, due to a higher average CO_2 intensity of the network.

It is also interesting to analyze the time history of the aviation-induced ΔT, shown in Figure 14. Plot (a) shows the temperature increase linked to 30 years of operations of the jet fuel fleet, which sees the biggest contributors being NO_x, AIC, and CO_2, which remain in the atmosphere even once operations are concluded. The peak of temperature change is at the end of the operational period of 30 years. Plot (b) shows the temperature increase linked to the legacy fleet, which, coupled with plot (c) showing the climate impact of hydrogen aircraft, details the impact of the analyzed transient. It is interesting to notice that the shape of the total impact of the reference and of the hydrogen cases is similar, with a peak at 30 years. Instead, the progressive reduction in the jet fuel fleet shows an interesting behavior, with a global peak at 11 years from the beginning of the operations and a local peak at the end of the 30-year period, mostly due to CO_2. At last, plot (d) puts into scale the reference and the two transient scenarios, showing how positive the introduction of hydrogen aircraft is on the aviation-induced temperature increase.

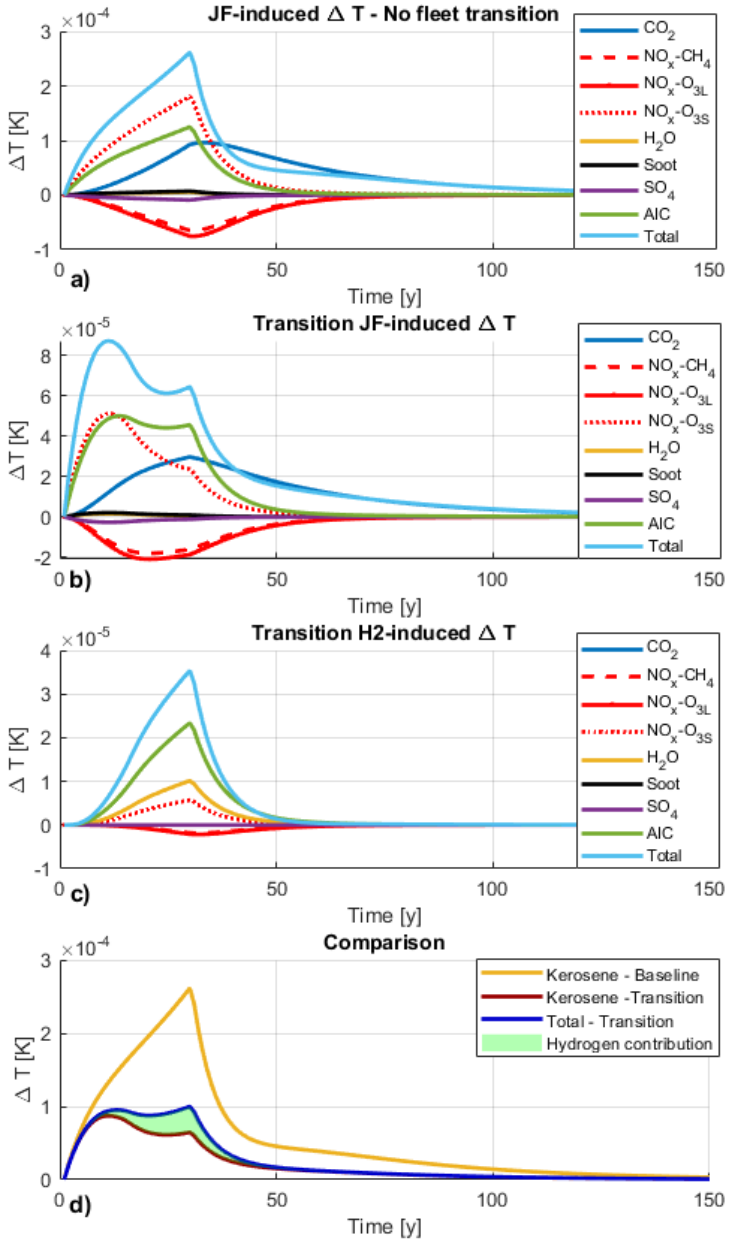

Figure 14. ΔT response: (**a**) Baseline scenario, (**b**) JF impact in fleet transition, (**c**) H_2 in fleet transition and (**d**) comparison of the three.

Furthermore, it is necessary to perform a sensitivity study on the reduction in the AIC RF per unit distance for hydrogen aircraft, as the −70% figure is not justified in [14]. The reference RF per unit distance for kerosene aircraft is varied within a ±70% range to account for possible deviations. Results, shown in Figure 15, show the temperature increase due to AIC emitted by hydrogen aircraft, normalized by the ΔT in the transition scenario (blue), which varies with the variation of the RF, and by the constant ΔT of the reference scenario with kerosene aircraft only (red).

In the −70% case, considered in all the previous results, AIC emitted by hydrogen aircraft contributes only minimally to the estimated temperature increase, at 6% of the reference, going up to 34% in the most extreme scenario. Thus, the uncertainty on the RF per unit distance of hydrogen aircraft causes the potential temperature increase mitigation to vary between −57% and −30%, showing how more detailed analysis on contrail modeling, and eventual operational mitigation, are required. The last caveat on the proposed climate impact modeling of contrail concerns the high dependency on atmospheric conditions of contrail formation and radiative forcing, which at given conditions can also have a cooling effect on the Earth atmosphere. In this work, which considers large operational scenarios consisting of full airline networks over a 30-year period, it is necessary to consider an average RF for contrails, of both hydrogen and kerosene aircraft, whereas the analysis of single trajectories can achieve higher accuracy of contrail formation and impact modeling, thanks to the introduction of local weather conditions (temperature, humidity, wind, time of emission and others).

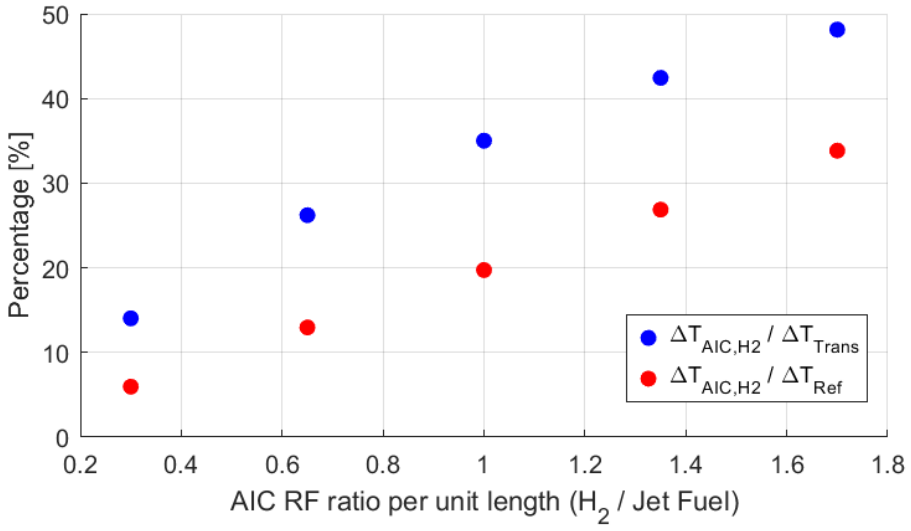

Figure 15. Sensitivity studies on the impact.

5. Conclusions

The paper shows the impact of operations of a short- and medium-range fleet transitioning from jet fuel to hydrogen propulsion, considering the constraint arising from the availability of hydrogen refueling infrastructures and the intrinsic difference in performance between the two sub-fleets.

This study first formulates a minimization problem to assess the operational impact of hydrogen availability at airports within a specified airline network. The analysis accounts for aircraft with distinct design ranges and introduces the possibility to serve shorter flights recurring to tankering. This work introduces the novel concept of maximum range for single refueling return trips, defining the farthest return distance an aircraft can achieve by refueling only at its departure airport and tankering hydrogen for the return leg—while accounting for regulatory reserves for both segments. This approach enables hydrogen-

powered aircraft to operate at airports lacking hydrogen refueling infrastructure, as long as the distance from a hydrogen-equipped hub remains within this calculated range. The analysis of the design range of a hydrogen aircraft, based on the TLARs of the Airbus A320, shows that, for European short-haul networks and with a set availability of hydrogen at airports, a reduced design range of 2450 km enables sufficient network coverage, spanning between 81% and 96%, while reducing the negative impact arising from the integration of the novel fuel within the airframe.

With the introduction of a fleet replacement model, it becomes evident that the number of routes potentially serviceable by hydrogen-powered aircraft exceeds the available fleet size, especially right after the EIS of the novel fleet. This creates an opportunity to optimize aircraft assignments between conventional and hydrogen sub-fleets, enhancing operational efficiency. In fact, the hydrogen and jet fuel sub-fleets can be assigned to routes, with the ambition of minimizing specific criteria, such as CO_2 or energy intensity, or FCASK. Minimum energy solutions assign the shortest routes to the hydrogen sub-fleet, whereas the other two exploit the full capabilities of the novel aircraft. As the fleet transition progresses, with hydrogen aircraft accounting for up to 77% of total flight hours, the potential reduction in the network-induced temperature increase goes up to 57.4%, as quantified by the ATR indicator applied only to tank-to-wake emissions, thus implying the usage of green hydrogen. This marks the significant climate mitigation benefits of adopting hydrogen-powered aviation. The presented methodology could be improved by introducing a time-evolving hydrogen refueling infrastructure scenario, in order to assess how impactful this constraint would be along the transition. Furthermore, airline data detailing passenger numbers could be included to refine the model to account for aircraft of different sizes as well.

This article is a revised and expanded version of a paper [21] entitled "TRANSIENT IN OPERATIONS: FROM JET-FUEL TO HYDROGEN-POWERED AIRCRAFT", which was presented at Towards Sustainable Aviation Summit (TSAS), Toulouse, France, 2025.

Author Contributions: Conceptualization, G.S.; Methodology, G.S.; Resources, L.T.; Data curation, G.S.; Writing—original draft, G.S.; Writing—review & editing, L.T.; Supervision, L.T.; Funding acquisition, L.T. All authors have read and agreed to the published version of the manuscript.

Funding: This research received no external funding.

Data Availability Statement: The original contributions presented in the study are included in the article, further inquiries can be directed to the corresponding author.

Conflicts of Interest: The authors declare no conflicts of interest.

References

1. Air Transport Action Group. Facts and Figures. 2020. Available online: https://www.atag.org/facts-figures/ (accessed on 20 December 2024).
2. Adler, E.J.; Martins, J.R. Hydrogen-powered aircraft: Fundamental concepts, key technologies, and environmental impacts. *Prog. Aerosp. Sci.* **2023**, *141*, 100922. [CrossRef]
3. Debney, D.; Beddoes, S.; Foster, M.; Darren, J.; Kay, E.; Kay, O.; Shawki, K.; Stubbs, E.; Thomas, D.; Weider, K.; et al. Zero-Carbon Emission Aircraft Concepts. 2022. Available online: https://www.ati.org.uk/wp-content/uploads/2022/03/FZO-AIN-REP-0007-FlyZero-Zero-Carbon-Emission-Aircraft-Concepts.pdf (accessed on 1 September 2025).
4. Eissele, J.; Lafer, S.; Mejía Burbano, C.; Schließus, J.; Wiedmann, T.; Mangold, J.; Strohmayer, A. Hydrogen-Powered Aviation—Design of a Hybrid-Electric Regional Aircraft for Entry into Service in 2040. *Aerospace* **2023**, *10*, 277.
5. Airbus. *ZeroE: Towards the World's First Zero Emission Aircraft*; Airbus: Blagnac, France, 2020.
6. Gundry, K. Universal Hydrogen Successfully Completes First Flight of Hydrogen Regional Airliner. *Business Wire*, 2 March 2023.
7. Avia, Z. ZeroAvia Receives FAA Signed P-1 for 600kW EPS. 2025. Available online: https://zeroavia.com/press/zeroavia-receives-faa-signed-p-1-for-600kw-eps/ (accessed on 1 September 2025).

8. Sampson, B. What Next for Hydrogen-Electric Aircraft. 2025. Available online: https://www.aerospacetestinginternational.com/features/what-next-for-hydrogen-electric-aircraft.html (accessed on 1 September 2025).
9. European Commission. Directorate General for Climate Action. *Going Climate-Neutral by 2050: A Strategic Long Term Vision for a Prosperous, Modern, Competitive and Climate Neutral EU Economy*; Publications Office: Luxembourg, 2019.
10. European Commission. *Reducing Emissions from Aviation*; European Commission: Luxembourg, 2025.
11. European Commission. *RefuelEU Aviation Initiative: Council Adopts New Law to Decarbonise the Aviation Sector*; European Commission: Luxembourg, 2025.
12. Barton, D.; Hall, C.; Oldfield, M. Design of a Hydrogen Aircraft for Zero Persistent Contrails. *Aerospace* **2023**, *10*, 688. [CrossRef]
13. Hoelzen, J.; Silberhorn, D.; Schenke, F.; Stabenow, E.; Zill, T.; Bensmann, A.; Hanke-Rauschenbach, R. H2-powered aviation—Optimized aircraft and green LH2 supply in air transport networks. *Appl. Energy* **2025**, *380*, 124999. [CrossRef]
14. Proesmans, P.; Vos, R. Hydrogen, medium-range airplane design optimization for minimal global warming impact. *CEAS Aeronaut. J.* **2024**, *15*, 781–806. [CrossRef]
15. Mukhopadhaya, J.; Rutherford, D. Performance analysis of evolutionary hydrogen-powered aircraft. *Int. Counc. Clean Transp.* **2022**. Available online: https://theicct.org/publication/aviation-global-evo-hydrogen-aircraft-jan22/ (accessed on 1 September 2025).
16. Kotzem, M.; Wöhler, S.; Burschyk, T.; Hesse, C.; Hellbrück, S. Conceptual aircraft design of a research baseline with direct liquid hydrogen combustion. In Proceedings of the 34th ICAS Congress, Firenze, Italy, 9–13 September 2024.
17. Healy, F.; Gu, H.; Rezgui, D.; Cooper, J. Conceptual design of hydrogen-powered aircraft: High aspect ratio wings and floating wingtips. In Proceedings of the 34th ICAS Congress, Firenze, Italy, 9–13 September 2024.
18. Onorato, G.; Proesmans, P.; Hoogreef, M.F.M. Assessment of hydrogen transport aircraft: Effects of fuel tank integration. *CEAS Aeronaut. J.* **2022**, *13*, 813–845. [CrossRef] [PubMed]
19. Verstraete, D. On the energy efficiency of hydrogen-fuelled transport aircraft. *Int. J. Hydrogen Energy* **2015**, *40*, 7388–7394. [CrossRef]
20. Trainelli, L.; Riboldi, C.E.D.; Sirtori, G. Methodologies for the Preliminary Sizing of Hydrogen-Powered Aircraft and Supporting Airport Infrastructures. In Proceedings of the 34th ICAS Congress, Firenze, Italy, 9–13 September 2024.
21. Sirtori, G.; Trainelli, L. Transient in Operations: From Jet-Fuel to Hydrogen-Powered Aircraft. In Proceedings of the Towards Sustainable Aviation Summit (TSAS 2025), Toulouse, France, 28–30 January 2025. [CrossRef]
22. Barry, N.; Gallagher, C.; Stuart, C.; Fitzgerald, S. Optimizing for sustainability as an objective function within airline fleet scheduling: An Ireland—EU mobility case study. In Proceedings of the AIAA Aviation Forum and Ascend 2024, Las Vegas, NV, USA, 29 July–2 August 2024. [CrossRef]
23. Botero, M.; Wendorff, A.; MacDonald, T.; Variyar, A.; Vegh, J.; Lukaczyk, T.; Alonso, J.; Orra, T.; Ilario Da Silva, C. SUAVE: An Open-Source Environment for Conceptual Vehicle Design and Optimization. In Proceedings of the 54th AIAA Aerospace Sciences Meeting, San Diego, CA, USA, 4–8 January 2016. [CrossRef]
24. Hoelzen, J.; Flohr, M.; Silberhorn, D.; Mangold, J.; Bensmann, A.; Hanke-Rauschenbach, R. H2-powered aviation at airports—Design and economics of LH2 refueling systems. *Energy Convers. Manag.* **2022**, *14*, 100206. [CrossRef]
25. Hoelzen, J.; Silberhorn, D.; Schenke, F.; Stabenow, E.; Zill, T.; Bensmann, A.; Hanke-Rauschenbach, R. H2-powered aviation—Optimized aircraft and green LH2 supply in air transport networks. *Preprint* **2023**, SSRN:4613255.
26. Scott, M.; Clarke, H. *Analysing the Costs of Hydrogen Aircraft*; Final Report; Transport & Environment: Brussels, Belgium, 2023.
27. Gronau, S.; Hoelzen, J.; Mueller, T.; Hanke-Rauschenbach, R. Hydrogen-powered aviation in Germany: A macroeconomic perspective and methodological approach of fuel supply chain integration into an economy-wide dataset. *Int. J. Hydrogen Energy* **2023**, *48*, 5347–5376. [CrossRef]
28. Royal, N. *Novel Propulsion and Alternative Fuels for Aviation Towards 2050*; Netherlands Aerospace Centre NLR: Leiden, The Netherlands, 2022.
29. ATAG. *WAYPOINT 2050*; ATAG: Geneva, Switzerland, 2020.
30. IEA. Energy Technologies Perspectives. 2006. Available online: https://www.iea.org/reports/energy-technology-perspectives-2006 (accessed on 1 September 2025).
31. Oesingmann, K.; Grimme, W.; Scheelhaase, J. Hydrogen in aviation: A simulation of demand, price dynamics, and CO_2 emission reduction potentials. *Int. J. Hydrogen Energy* **2024**, *64*, 633–642. [CrossRef]
32. Schwartz Dallara, E.; Kroo, I.; Waitz, I. Metric for Comparing Lifetime average Climate Impact of Aircraft. *AIAA J.* **2011**, *49*, 1600–1613. [CrossRef]
33. Russell, C.; Johnson, W. Application of Climate Impact Metrics to Rotorcraft Design. In Proceedings of the AIAA Aerospace Sciences Meeting, Grapevine, TX, USA, 7–10 January 2013.
34. Bock, L.; Burkhardt, U. Contrail cirrus radiative forcing for future air traffic. *Atmos. Chem. Phys.* **2019**, *19*, 8163–8174.

35. Lee, D.S.; Fahey, D.W.; Skowron, A.; Allen, M.R.; Burkhardt, U.; Chen, Q.; Doherty, S.J.; Freeman, S.; Forster, P.M.; Fuglestvedt, J.; et al. The contribution of global aviation to anthropogenic climate forcing for 2000 to 2018. *Atmos. Environ.* **2021**, *244*, 117834. [CrossRef] [PubMed]
36. Winher, M.; Rypdal, K. *EMEP/EEA Air Pollutant Emission Inventory Guidebook 2019, Aviation*; European Environment Agency: Copenhagen, Denmark, 2019.
37. Sánchez-Bastardo, N.; Schlögl, R.; Ruland, H. Methane Pyrolysis for Zero-Emission Hydrogen Production: A Potential Bridge Technology from Fossil Fuels to a Renewable and Sustainable Hydrogen Economy. *Ind. Eng. Chem. Res.* **2021**, *60*, 11855–11881. [CrossRef]
38. Ji, M.; Wang, J. Review and comparison of various hydrogen production methods based on costs and life cycle impact assessment indicators. *Int. J. Hydrogen Energy* **2021**, *46*, 38612–38635. [CrossRef]
39. Aigner, B.; Garcia Garriga, A.; Sirtori, G.; Riboldi, C.E.D.; Trainelli, L.; Mariani, C.; Mancini, M. Overview and preliminary results of the scalability investigation of hybrid Electric concepts for next-generation aircraft (SIENA) project. In *Journal of Physics: Conference Series*; IOP Publishing: Bristol, UK, 2023.
40. EUROCONTROL. Fuel Tankering: Economic benefits and environmental impact. In *Aviation Intelligence Unit, Think Paper 1*; EUROCONTROL: Brussels, Belgium, 2019.
41. Fox, J.; Weisber, S. *Nonlinear Regression and Nonlinear Least Squares in R*; SAGE Publications, Inc.: Thousand Oaks, CA, USA, 2010.
42. EUROCONTROL. Data Snapshot: Average Flight Distance in 2020. 2021. Available online: https://www.google.com/url?sa=t&source=web&rct=j&opi=89978449&url=https://www.eurocontrol.int/sites/default/files/2021-04/eurocontrol-data-snapshot-9-average-flight-2020.pdf&ved=2ahUKEwiNh9rNkKSGAxU3S_EDHRggBjUQFnoECBcQAQ&usg=AOvVaw0J1xzym-3uGUdPNf0PEYdo (accessed on 20 February 2024).
43. HORIZON Europe. Environmentally Friendly Aviation for all Classes of Aircraft. 2023. Available online: https://cordis.europa.eu/project/id/101056866 (accessed on 20 February 2024).
44. Eurocontrol. *Daily Traffic Variation—Airport 2023*; EUROCONTROL: Brussels, Belgium, 2023.
45. SEA Milan Airports. Sustainability Report 2022. 2022. Available online: https://milanairports.com/en/sustainability-report-2022 (accessed on 20 February 2024).
46. easyJet. Annual Report 2022. 2022. Available online: https://s203.q4cdn.com/522538739/files/shareholder_docs/2023/annual-report-2022.pdf (accessed on 20 January 2024).
47. Flight Labs. *Flight Labs API*; Flight Labs: Adelaide, SA, USA, 2023.
48. Morrel, P.; Dray, L. *Environmental Aspects of Fleet Turnover, Retirement and Life Cycle*; Final Report; Omega, Aviation in a Sustainable World; 2009.
49. Viry, P.; Planès, T.; Delbecq, S.; Joly, L.; Salgas, A. An empirical and customisable fleet renewal model for prospective scenarios using open-access data. In Proceedings of the 34th ICAS Congress, Firenze, Italy, 9–13 September 2024.
50. Ozdemir, Y.; Basligil, H.; Sarsenov, B. A Large Scale Integer Linear Programming to the Daily Fleet Assignment Problem: A Case Study in Turkey. *Procedia Soc. Behav. Sci.* **2012**, *62*, 849–853. [CrossRef]
51. ReVelle, C.; McGarity, A. *Design and Operation of Civil and Environmental Engineering Systems*; John Wiley & Sons: New York, NY, USA, 1997.
52. Valenduc, C. The carbon pricing proposals of the 'Fit for 55' package: An efficient and fair route to carbon neutrality. *SSRN Electron. J.* **2022**. [CrossRef]
53. Icelandair. Consolidated Financial Statements for the Year 2023. Available online: https://assets.contentstack.io/v3/assets/blt7c94950eb7f3edcb/blt90e4ab140db5669f/65bcef2ed6cf04846a150690/consolidated-financial-statement-for-year-2023-icelandair-gr.pdf (accessed on 1 September 2025).
54. AEROPORTI. 2030. Italian Airport Traffic Data. Available online: https://www.aeroporti2030.com/airport-traffic-data/ (accessed on 1 September 2025).
55. Eurocontrol. Forecast Update 2024–2030. 2024. Available online: https://www.eurocontrol.int/publication/eurocontrol-forecast-2024-2030-autumn-update (accessed on 1 September 2025).